Desalination and Water Treatment
www.deswater.com
doi: 10.5004/dwt.2021.27281

226 (2021) 137–146
June

Catalytic destruction of 2,4-D in aqueous environment using transition metal-doped ZnO nanoparticles under ultrasonic waves, UV and visible light

Roya Ebrahimi[a], Afshin Maleki[a,*], Kazem Godini[a], Reza Rezaee[a], Ali Jafari[b], Seung-Mok Lee[c,*], Jeong Hyub Ha[d,*]

[a]*Environmental Health Research Center, Research Institute for Health Development, Kurdistan University of Medical Sciences, Sanandaj, Iran, emails: maleki43@yahoo.com (A. Maleki), ebrahimi83@yahoo.com (R. Ebrahimi), kazem_goodyny@yahoo.com (K. Godini), rezaee.eng@gmail.com (R. Rezaee)*
[b]*Department of Environmental Health Engineering, Faculty of Health and Nutrition, Lorestan University of Medical Sciences, Khorramabad, Iran, email: jafari_a99@yahoo.com*
[c]*Department of Environmental Engineering, Catholic Kwandong University, Ganeung, 25601, Korea, email: leesm@cku.ac.kr*
[d]*Department of Integrated Environmental System, Pyeongtaek University, Pyeongtaek, 17869, Korea, email: jhha@ptu.ac.kr*

Received 18 October 2020; Accepted 1 April 2021

ABSTRACT

This study investigated the performance of photocatalytic and sonocatalytic processes using zinc oxide nanoparticles doped with copper and cerium for the degradation of 2,4-dichlorophenoxyacetic acid (2,4-D) as a commonly used herbicide in wheat and barley cultivation. The doped metal nanoparticles were synthesized by the thermal solvent method using zinc nitrate precursor and metal salts. The synthesized nanoparticles were characterized using scanning electron microscopy, X-ray diffraction, Fourier-transform infrared spectroscopy, atomic force microscopy, dynamic light scattering and zeta potential analyses. According to the results, the Ce.ZnO nanoparticles, in the presence of visible light, yielded the highest removal efficiency (87%) in removing herbicide. Therefore, in this study, the Ce.ZnO nanoparticles were used as the most effective nanoparticles in the next experiments. The results indicated that the photocatalytic process had the highest herbicide removal efficiency at neutral solution pH. Moreover, raising Ce.ZnO nanoparticle dose increased the photocatalytic removal efficiency of the herbicide. It was found that the photocatalytic efficiency increased with raising contact time. In contrast, increasing the initial 2,4-D concentration caused the efficiency to decline. It can be concluded that the Ce.ZnO nanoparticles, in the presence of visible light, can be efficiently utilized for the removal of 2,4-D herbicide from aqueous solutions.

Keywords: Zinc oxide; Contaminants; Herbicides; Intermediate metals

1. Introduction

Over the past few decades, the use of chemical pesticides in agriculture has been on the rise dramatically and their residues in agricultural products have become a major concern worldwide [1,2]. This widespread application of pesticides has resulted in an increase in the residual concentration of these toxic compounds in surface and groundwaters [3–5]. 2,4-dichlorophenoxyacetic acid (2,4-D), as one of the most widely employed herbicides is a selective herbicide to control broadleaf weeds, especially in wheat and barley cultivation. Due to the high water solubility, high stability and low biological degradability, this compound has received much attention from researchers worldwide. It is generally formulated as in salt, amine

* Corresponding authors.

and ester formulations that are commercially available [4]. After application of 2,4-D in agriculture, owing to its high solubility in water (600 mg/L at 25°C), it can easily leach through the soil and potentially reach groundwater [6]. Therefore, after a prolonged period of inappropriate use of 2,4-D, it may be found in surface and groundwaters at different concentrations [7]. Previous studies in the US and European countries reported the presence of various contents of herbicides such as atrazine, cyanisine, simazine, alachlor, metolachlor and chlorophenoxy acids including 2,4-D in surface and groundwaters [8]. In a study, 17 types of herbicides, which their concentrations were higher than the maximum allowable level recommended by the Environmental Protection Agency (EPA), were identified in drinking water in the US, [9]. Therefore, it is necessary to implement control and management programs for the use of these herbicides.

To date, several methods, such as ultrasonic waves [10], biodegradation [11], photodegradation, gamma radiation, photocatalytic processes [12], have been applied for the degradation of agricultural herbicides. Most of these methods suffer from many drawbacks like complexity, low degradation rate, high cost and chemical need, sludge production, which limit their large-scale applications [13]. In recent decades, photocatalytic processes have received much interest for the degradation of persistent pollutants from water and wastewater [14]. In this regard, a variety of photocatalysts (e.g., SnO_2, WO_3, Fe_2O, ZnO, CdS, $SrTiO_3$, ZnS and TiO_2) have been used in photocatalyst processes for the treatment of water and wastewater containing organic pollutants [15–19]. However, most of these materials are not applicable in the presence of ultraviolet (UV) irradiation, because it can lead to the agglomeration of their particles. Hence, doping has recently been introduced as an appropriate approach to solve this problem [16]. In this approach, dopants and surface modifiers are employed to reduce the energy gap, thereby enabling nanocrystal to be activated under visible light irradiation, which can prevent clogging and adhesion of nanocrystal structure [20]. The combination of metal oxides with nanoparticles has attracted much interest from many researchers in various fields such as chemistry, physics, environmental and materials sciences [16]. One of the most important advantages of this technology is its high sensitivity due to the larger specific surface area of the crystals used. The quantum size effect is another plus factor of the doping technology, which decreases the particle size from a critical state and separates the valence layer and conduction layer. Therefore, in the doped catalyst, the electrical potential of the valence layer is more positive and the electrical potential of the conduction layer is negative, which causes an increase in the oxidation capacity of the catalyst [21]. Hence, in order to increase the adsorption of visible irradiation, ultrasonic waves and activation of the catalyst by power sources, the ZnO bandgap is divided into several sub-gaps by doping through metal or non-metallic ions, which results in easier activation with lower energy [22].

Currently, there are few reports of copper doped and cerium doped ZnO nanocomposites for photocatalytic applications as well as 2,4-D decomposition by doped nano-catalysts in water. However, based on our comprehensive literature review, there are no research studies on the sono and photocatalytic degradation of 2,4-D by cerium and copper doped ZnO nanocatalysts synthesized by the hydrothermal method. In addition, the optimal values of the effective parameters in this process have been paid less. Therefore, in this study, two elements, copper and cerium, were selected because previous research has shown that cerium has a strong effect on the structural properties of ZnO nanorods, strong absorption and emission in a visible region of UV-vis and PL spectra [23]. In the same way, copper is an inexpensive element and its size is close to Zn, so Cu^{2+} can be easily incorporated into the crystal structure of ZnO and shift the absorption and emission spectra to the visible light region [24]. Due to the importance of the subject, therefore, the present research focuses on the synthesis of Cu-doped and Ce-doped ZnO nanoparticles by hydrothermal method and aims to determine their efficacy in the degradation of 2,4-D under ultraviolet irradiation, ultrasound radiation and visible light illumination. The effect of solution pH, catalyst dose, initial concentration of 2,4-D, and contact time on the degradation process of 2,4-D and optical properties of nanoparticles was also investigated.

2. Materials and methods

2.1. Chemicals

In this study, 2,4-D was purchased from Meshkfam Chemical Co., (Iran). Other chemicals including zinc nitrate hexahydrate, oxalic acid, cerium salt, sulfuric acid and nitric acid were provided by Merck & Co., (Germany).

2.2. Preparation of zinc oxide nanoparticles doped with cerium and copper metals

To synthesize the nanoparticles, a certain amount of zinc nitrate hexahydrate solution (0.4 mM) and oxalic acid (0.6 mM) in ion-free water was separately heated to the boiling point and then mixed with zinc nitrate solution. The oxalic acid solution was added into this mixture to form an oxalate precipitate (as solution 1). Next, cerium salt was stirred and heated to 60°C–70°C for 1 h (as solution 2). The solutions were then cooled to room temperature. The Ce-Zinc crystals were washed several times with distilled water and then dried at 100°C for 5 h. Afterwards, the dried samples were calcined in a furnace at 450°C for 12 h [15]. Oxide and copper nano-catalysts were prepared according to the described method. Pure ZnO was also prepared without adding contaminant salts.

2.3. Characterization of the prepared nanocatalyst

Fourier-transform infrared spectroscopy (FTIR; Tensor 27 spectrophotometer, Bruker, Germany) was employed for the examination of chemical bonds and surficial functional groups on the Cu-doped ZnO nanoparticles. The surface morphology of the catalyst samples was characterized by scanning electron microscopy (SEM) (Zeiss, Germany). And, the X-ray diffraction (XRD) of Cu-doped ZnO was recorded using a powder diffractometer (Bruker ARSD8 Advance) equipped with a Cu K radiation source at a wavelength of 150 nm.

2.4. Photocatalyst experiments

In this study, a batch flow reactor was used for the photocatalytic experiments. The reactor was made up of glass with a cylindrical shape. Three 6-W low-pressure UVC lamps were applied as UV irradiation. The lumps were embedded on the top of the reactor. The distance between the UV lamps and the surface of the immobilized synthesized nanocatalyst was 1 cm. Moreover, in order to mix the solution in the reactor, a magnetic stirrer (Heidolph, Germany) was used. In the next step, the experiments were conducted under visible light. For this reason, the reactor containing 2,4-D and the prepared nanocatalyst was exposed to sunlight to provide visible irradiation. At this stage, the experiments were performed on sunny days during the August month of 2019 in the city of Sanandaj, Iran (35°20′N 46°50′E). In this study, in order to determine the efficacy of the synthesized nanoparticles for degradation of 2,4-D in the presence of ultraviolet irradiation, visible light and ultrasound waves, the experiments were conducted at an initial 2,4-D concentration of 10 mg/L, nanoparticle dose of 0.15 g/L and natural solution pH. Next, the effect of different pH values of 3, 5, 7, 9 and 11 was investigated on the removal of the herbicide in the presence of visible light. Afterward, to investigate the effect of the synthesized nanoparticles on herbicide removal efficiency, the experiments were conducted at five nanoparticle doses of 0.05, 0.1, 0.15, 0.2 and 0.25 g/L in the presence of visible light. Moreover, the effect of contact time in the photocatalytic process in the presence of visible light was studied at various contact times (30–150 min).

2.5. Sonocatalytic experiments and analysis

In this step, the ultrasonic bath was used for the sonocatalytic experiments. In this regard, 100-mL flasks were placed in an ultrasonic bath. After adjusting pH, the synthesized nanoparticles were added and irradiated with ultrasonic waves. After sonocatalytic reaction, the residual concentrations of 2,4-D were determined at different times. The sonocatalytic process was performed at a frequency of 37 kHz.

In the present research, the concentrations of the herbicide in the samples were measured using a spectrophotometer (DR5000-HACH) at a 280-nm wavelength after the reaction.

3. Results and discussion

3.1. Characterization of the prepared nanocatalyst

Fig. 1 presents the SEM images of the zinc oxide nanoparticles doped with cerium and copper metals with a magnification of 500 nm. As observed, the size of the nanoparticles was determined using SEM by Digimizer software. In the SEM mages, the nanoparticles on the catalyst surface may appear bulky due to their small size. The SEM images showed that the appearance of the nanoparticles was hexagonal, indicating the presence of zinc oxide [25].

XRD spectroscopy provides information on the structures, phases and preferred crystal orientations of the prepared nanocatalyst. As shown in Fig. 2, the XRD spectra of the synthesized ZnO, Ce.ZnO and Cu.ZnO nanoparticles illustrate that there were three main peaks of (100), (002) and (101), respectively, which are consistent with the position of the zinc oxide peaks, corresponding to the standard JCPDS card (No. 800075). These patterns represent that the synthesized nanocatalyst had a hexagonal crystal structure. It was also observed that doping zinc oxide with the cerium and copper metals did not produce any additional peak and other reaction phases of the copper and cerium impurities. Doping with the mentioned metals and increasing their concentration caused a partial displacement of the diffraction peaks, which may be due to the larger ionic radius of

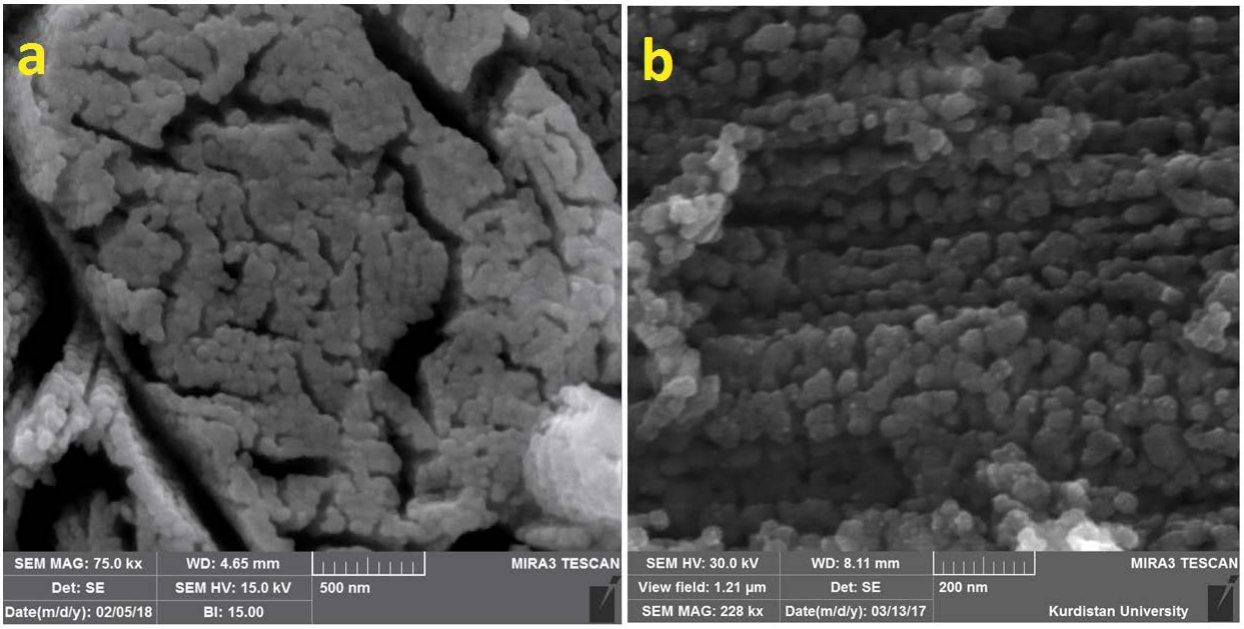

Fig. 1. SEM image of nanoparticles (a) Cu.ZnO and (b) Ce.ZnO.

these metals than Zn^{2+}. These doping metals are substituted at the zinc oxide crystal lattice sites and subsequently extend the crystalline lattice. The maximum intensities of the spectra were appeared at (101) at an angle of 2θ = 36.045 [26].

The FTIR spectra of the synthesized ZnO, Ce.ZnO, and Cu.ZnO nanoparticles indicate that a broad peak was observed at 469 cm^{-1} corresponding to the tensile frequency of Zn–O [22]. At 11,730 cm^{-1}, there was a C=O tensile bond that may be assigned to the presence of organic matter (Fig. 3). A peak at 13,000 cm^{-1} corresponds to C–H tensile bond that belongs to the amines group. Also, N–H tensile vibrations were shown at 3,448 cm^{-1}, which are assigned to the N–H tensile bond corresponding to the amines group [27]. These results are in agreement with the findings documented in a similar study on doping zinc oxide by means of chromium oxide. The appearance of peaks at 1,600–400 and 3,600–3,400 cm^{-2} confirms the existence of Zn–O tensile bond and N–H bond, respectively [28].

Atomic force microscopy detects near field forces between probe tip atoms and sample surface atoms rather than tunneling current. Fig. 4 shows the atomic force microscopy (AFM) analysis of the Ce.ZnO and Cu.ZnO nanoparticles. The surface topography images indicated the presence of the nanoparticles on the nanocatalyst surfaces. Moreover, d_x shows the size of the nanoparticles, which were 46 and 78 nm for the Ce.ZnO and Cu.ZnO nanoparticles, respectively. Furthermore, R_q expresses the relative roughness of the Ce.ZnO and Cu.ZnO nanoparticles, which were 1.0623 and 1696 nm, respectively.

Zeta potential can be used as a strong tool to study the potential distribution at the interface of colloids precisely. This experiment can also be conducted in the presence of simple ions and more complex systems such as surfactants, multivalent ions, polymers and even proteins. The zeta potential of the sample is commonly used to determine the tendency of the particles in the liquid to bond to each other. Fig. 5 shows the electrical potential of the synthesized nanocomposite. The results implied that doping of oxide nanoparticles increased the zeta potential and mobility of the nanoparticles. Thus, the zeta potential for the Cu.ZnO, Ce.ZnO and ZnO were –9.71, –11.75 and –10.66 mV, respectively.

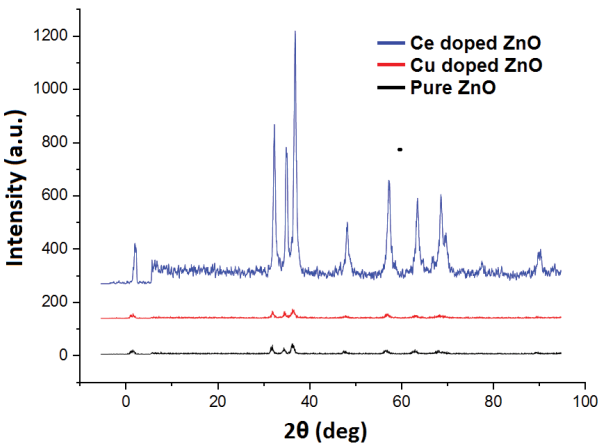

Fig. 2. X-ray diffraction spectra of the synthesized nanoparticles.

Dynamic light scattering as a physical method is used to determine the distribution of particles in solutions and suspensions. Dynamic light scattering as a fast and non-destructive measure is also applied to detect particle sizes in the range of a few micrometers to nanometers. In the current research, it was found that the cerium and copper doped ZnO nanoparticles had a smaller size and more uniform distribution than the pure zinc oxide.

3.2. Effect of the synthesized nanoparticles for removal of 2,4-D in the presence of ultraviolet irradiation, visible light and ultrasound

To determine the efficacy of the synthesized nanoparticles in degradation of 2,4-D in the presence of ultraviolet irradiation, visible light and ultrasound waves, the experiments were conducted at an initial 2,4-D concentration of 2.5 mg/L, nanoparticle dose of 0.15 g/L and natural solution pH. The results have been presented in Fig. 7. As can be seen, the highest removal efficiency in the photocatalytic process in the presence of visible light was achieved using the Ce.ZnO nanoparticles, which was 85%. Hence, the Ce.ZnO nanoparticles were used as the most effective nanoparticles in the next experiments. The higher efficiency of the Ce.ZnO nanoparticles may be attributed to the functional groups on the surface and the high relative roughness as presented in the AFM analysis. These characteristics improve the dispersion and absorption of the pollutants on the catalyst surface and subsequently cause an increase in the process efficiency [29]. In a similar study by Yıldırım et al. [30], the survey of the photocatalytic properties of the silver-doped ZnO showed that the optical and photocatalytic properties of the silver-doped ZnO were enhanced and more than the pure zinc oxide.

3.3. Effect of solution pH on the process efficiency

In this step, the effect of different pH values of 3, 5, 7, 9 and 11 was investigated on the removal of 2,4-D herbicide in the presence of visible light. The results showed

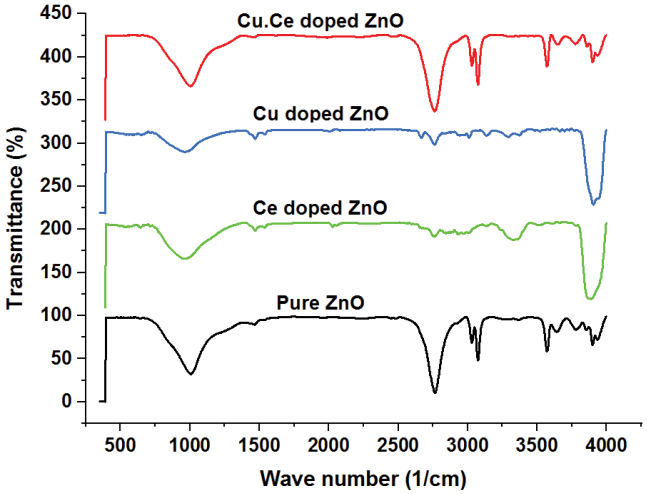

Fig. 3. Fourier transform infrared spectroscopy of the synthesized nanoparticles.

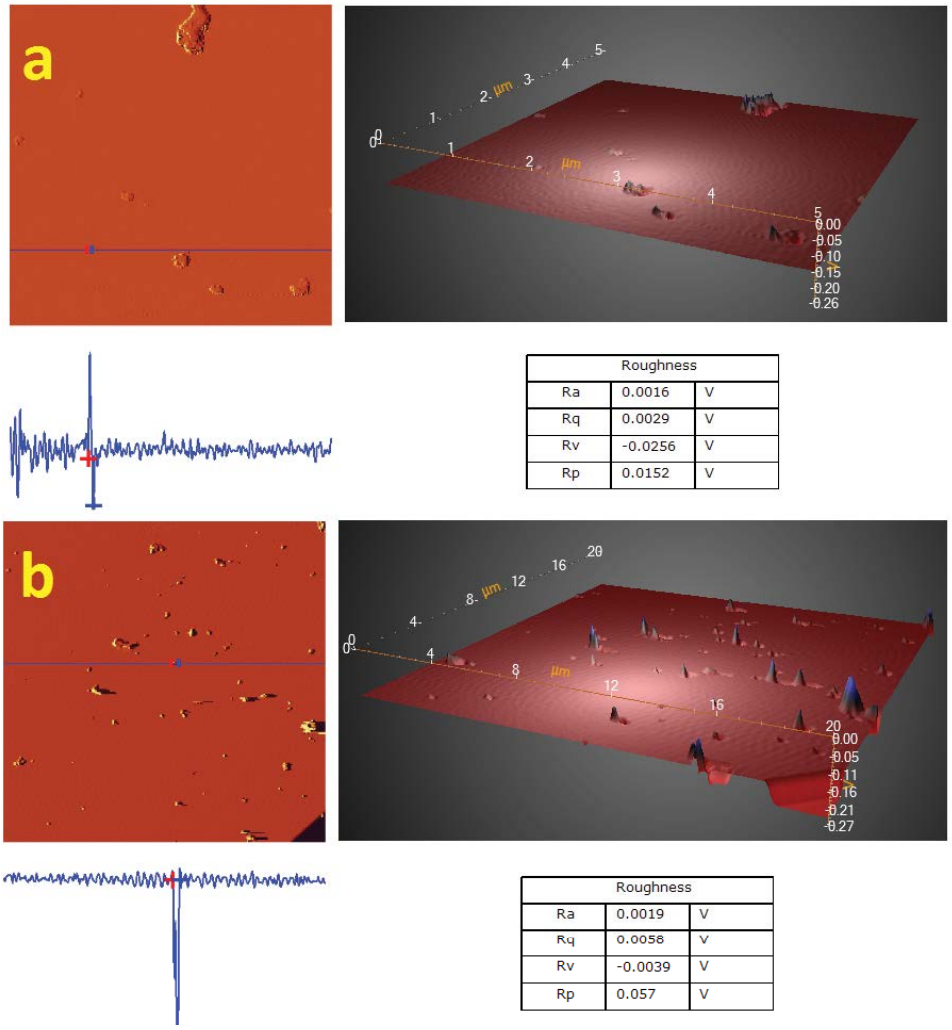

Fig. 4. AFM of (a) Cu.ZnO and (b) Ce.ZnO nanocomposite.

that the photocatalytic process efficiency in the presence of visible light at pH values of 3, 5, 7, 9 and 11 were 46%, 69%, 87%, 62% and 57%, respectively (Fig. 8). It was illustrated that the highest removal efficiency was obtained at the natural pH. For this reason, the optimum pH in this process was considered the natural value of the herbicide as the optimum pH. The reason for the increase in efficiency under these conditions can be stated that under these conditions the superoxide radical produced reacts with the hydrogen ion and produces hydroxyl radical. However, it is understandable that in alkaline conditions the rate of degradation is lower than that of acidic and neutral conditions, which can be attributed to the rapid decomposition of hydroxyl radicals [31]. Another factor affecting the solution pH can be assigned to the presence of higher levels of H^+ ions in the acidic medium followed by the formation of $OH^\bullet$ radicals [32].

3.4. Effect of synthesized nanoparticle dose on herbicide removal efficiency in the presence of visible light

To investigate the impact of the synthesized nanoparticle dose on herbicide removal efficiency, the experiments were conducted at five nanoparticle doses of 0.05, 0.1, 0.15, 0.2 and 0.25 g/L in the presence of visible light (Fig. 9). The results implied that raising the number of nanoparticles increased the herbicide removal efficiencies of 2,4-D, which were 18%, 39%, 85%, 88% and 95% at 0.05, 0.1, 0.15, 0.2 and 0.25 g/L of the nanoparticles, respectively, after 150 min of contact time. As observed in Fig. 8, with increasing the dosage of nanoparticle dose from 0.05 to 0.15 g/L, the process efficiency increased with a steep slope, but with further increasing dose from 0.15 to 0.25 g/L, it had a slight increase. Therefore, according to the results obtained, the optimum dose of the nanoparticles in photocatalytic of 2,4-D was considered to be 0.15 g/L. Previous studies have also reported that increasing the number of nanoparticles to a certain amount has a direct relationship with an increase in removal efficiency. It should be pointed out that further increase does not affect process efficiency and may even decrease the process efficiency because the suspended particles block the passage of light [33]. As previously mentioned, increasing the number of the nanoparticles increased the activation rate of the catalyst, thereby increasing the production rate of hydroxyl radicals and

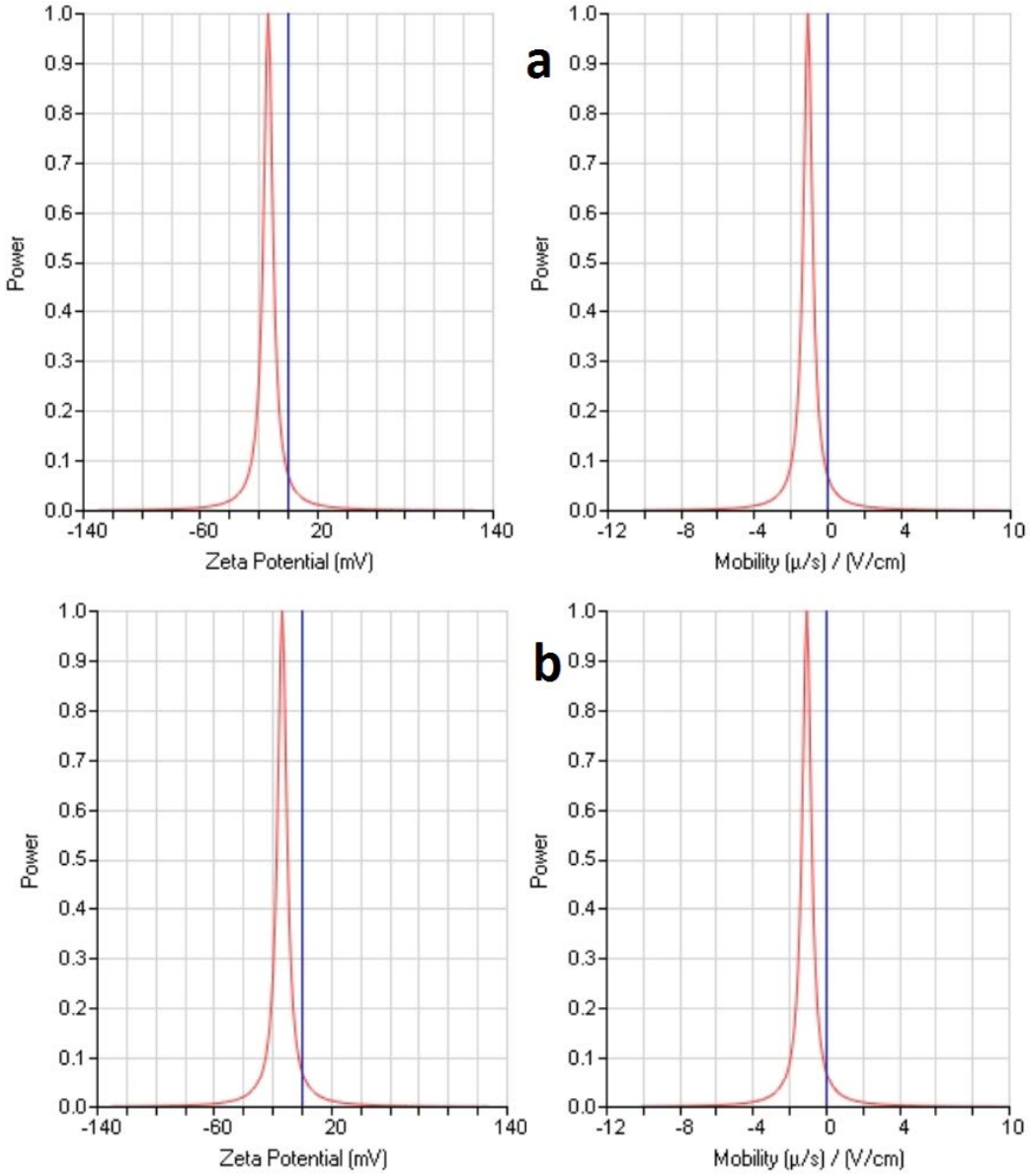

Fig. 5. Electrical potential of zeta nanoparticles (a) Cu.ZnO and (b) Ce.ZnO.

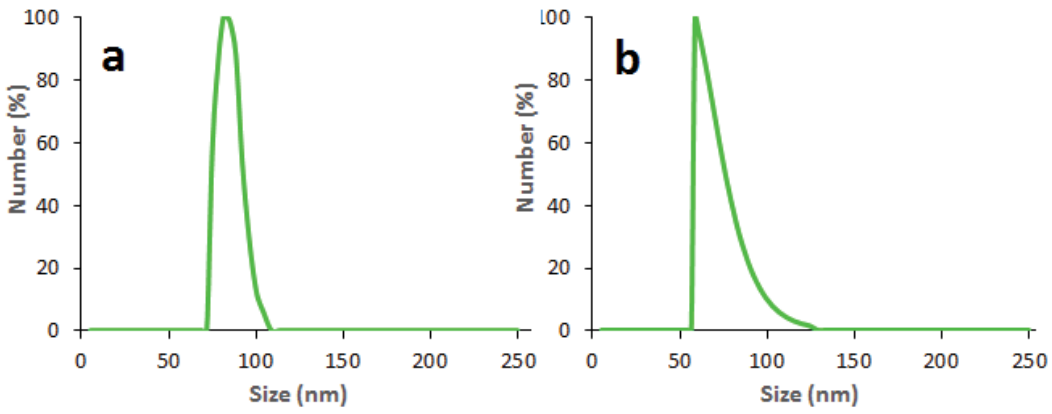

Fig. 6. DLS spectra of nanoparticles (a) Cu.ZnO and (b) Ce.ZnO.

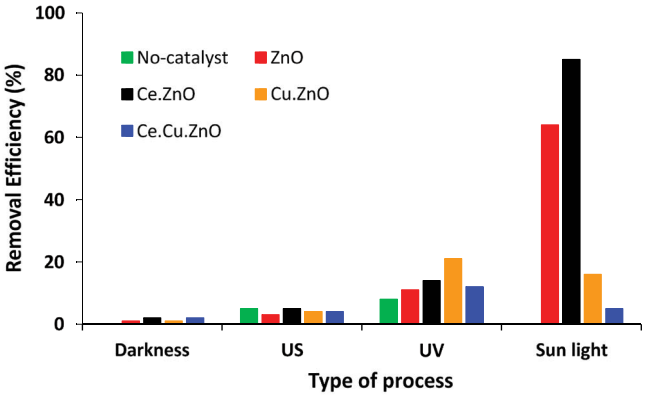

Fig. 7. Performance of the synthesized nanoparticles in 2,4-D removal.

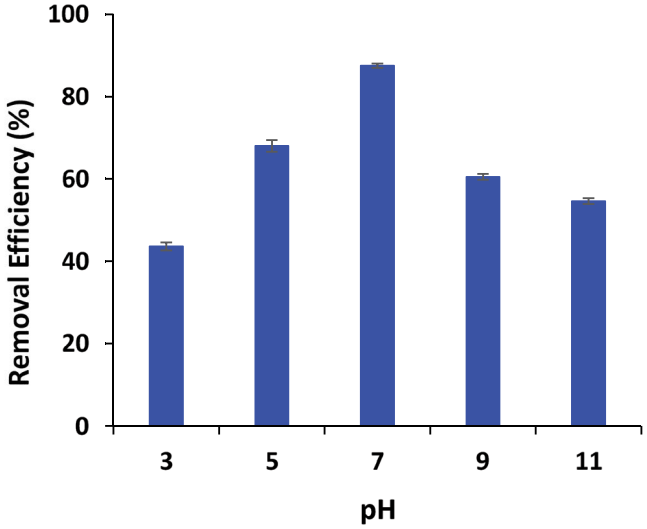

Fig. 8. Effect of pH on the process performance (initial 2,4-D concentration = 2.5 mg/L; Ce.ZnO dose = 0.15 g/L; time = 90 min; sunlight).

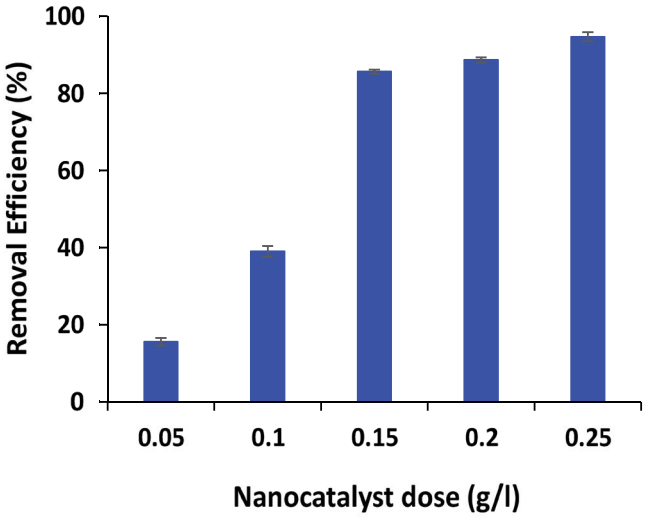

Fig. 9. Effect of nanoparticle dose on the process performance (initial 2,4-D concentration = 2.5 mg/L; Ce.ZnO dose = 0.15 g/L; time = 90 min; sunlight).

other oxidizing radicals [34]. Therefore, it can be concluded that an increase in nanoparticle dose has some positive effects on the photocatalytic process, while further increase can decrease the decomposition rate of the pollutant as a result of increasing the opacity and the scattering effect of light, which prevents the penetration of the visible light [35]. In the sonocatalytic process, ultrasonic waves generally act as an energy source for nanoparticle activation. Nanoparticles tend to aggregate due to their high surface area and high surface energy, but ultrasonic waves cause the nanoparticles to diffuse and not aggregate. However, when the number of nanoparticles exceeds a certain dose, the energy of ultrasonic waves is not sufficient to disperse them and therefore the removal efficiency remains constant as the concentration of nanoparticles increases [36].

3.5. Effect of initial 2,4-D concentration on the process performance in the presence of visible light

To investigate the effect of the initial concentration of herbicide on removal efficiency, the concentration of the herbicide at four levels of 2.5, 5, 7.5 and 500 mg/L in the presence of visible light was tested. In all the studied processes, increasing herbicide concentration caused the removal efficiency to decrease; the removal efficiencies of the process at 2,4-D concentrations of 2.5, 5, 7.5 and 500 mg/L were 83%, 72%, 68% and 63%, respectively, after 150 min of contact time in the presence of visible light (Fig. 10). This phenomenon may be attributed to the fact that by increasing the initial concentration of the contaminant, more catalyst surfactants are occupied, which causes a decrease in the production of oxidizing radicals and eventually results in a lower degradation rate of the target pollutant. High concentrations of pollutants absorb more UV photons, thereby declining the flux of UV photons for catalyst activation. Moreover, the lack of catalyst vacant sites reduces oxidant production and degradation rate [37]. Another probable reason for the decrease in the process efficiency with increasing 2,4-D may be owing to the occupation of vacant sites on the surface of the Ce.ZnO nanoparticles at high concentrations. According to Beer–Lambert's law, by increasing initial pollutant concentration, the pass rate of visible light and UV irradiation through the solution decreases, and by trapping and adsorbing on the dye particles, it reduces the absorption of photons by the photocatalyst, which results in a decrease in the production of the amount of active hydroxyl radicals, and hence the rate of decomposition decreases [38]. In many studies regarding the treatment of various pollutants by the ZnO photocatalytic process, it has been reported that the degradation efficiency decreases with increasing initial pollutant concentration [39]. It is worth noting that the photocatalyst performance and its degradation effect are directly related to the production of active hydroxyl radicals, which participate in the decomposition of the pollutants [40].

3.6. Effect of contact time on herbicide removal efficiency in the presence of visible light

The contact time in the photocatalytic process in the presence of visible light was studied at various contact times (30–150 min). The results showed that increasing time increased the herbicide removal efficiency. As can be seen, the removal efficiencies in the presence of visible light were 37%, 50%, 67%, 73%, 87%, 95%, 99%, 100% and 100%, respectively. Due to the fact that the collision of UV light with the catalyst surface leads to releasing the electron pair, and subsequently higher the number of electrons and thus the more hydroxyl radicals produced at higher contact item. Hence, the high concentrations of active hydroxyl radicals participate directly in the decomposition of herbicide molecules. As a result, the process efficiency increases with increasing reaction time. It should be noted that these observations are consistent with those of Ebrahimi et al. [27], on the removal of 2,4-D using the Mn-doped ZnO/graphene nanocomposite under LED radiation. In Table 1, the optimum conditions of the current research have been compared with other related studies.

3.7. Optical absorption and UV-Vis spectra

UV-Vis spectroscopy is a beneficial measure to display the potential of a semiconductor in absorbing light in a range of different wavelengths. Fig. 12 depicts the findings of the UV-Vis spectra of the pure ZnO nanoparticle and synthesized nanoparticles. The observations indicated that the optical absorption band of the pure ZnO was 380 nm with a bandgap of 3.25 eV. Hence, the pure ZnO could absorb light until 380 nm and any absorption did not happen in the visible light. However, the doping of the pure nanoparticle caused a change in the range of light absorption to longer and shorter wavelengths. It is because of the formation of the energy level of vacancy oxygen, as Ce and Cu contained in the zinc oxide crystal lattice can cause form vacancy oxygen [44,45]. The bottom line is that, in comparison with the pure ZnO, the synthesized nanoparticles of Ce.Cu-doped ZnO indicates redshift and is capable of absorbing longer wavelength. In accordance with our observations, Bharathi et al. [45] reported similar results.

3.8. Mineralization of 2,4-D

Regarding the chemical mechanisms of 2,4-D degradation, it is clear that the addition of Ce.ZnO strongly enhances the degradation of 2,4-D. The illumination of ZnO by sunlight excites electrons from the valence band and transfers them to the conduction band to generate electron–hole pairs [46]. Then the holes at the Ce.ZnO valence band can oxidize water or hydroxide to produce hydroxyl radicals. The hydroxyl radical is a strong oxidizing agent and therefore the photocatalytic degradation of 2,4-D produces various reaction intermediates under the influences of strong oxidants (mostly OH radicals) and electrons produced during photocatalysis reactions [46]. According to the available findings, 2,4-dichlorophenol, chlorophenol, phenol, hydroquinone, chlorohydroquinone, catechol, and maleic acid are the most important intermediates in the photocatalytic decomposition of 2,4-D. These intermediates react with hydroxyl radicals to produce final products (CO_2, H_2O and Cl) [47].

4. Conclusion

In this study, the efficiency of photocatalytic removal of 2,4-D herbicide in the presence of visible light and UV irradiation and ultrasound waves was investigated using zinc oxide nanoparticles doped with cerium and copper metals. For this reason, ZnO nanoparticles were first synthesized and then doped with cerium (Ce.ZnO) and copper metals (Cu.ZnO). The synthesized nanocatalyst was characterized

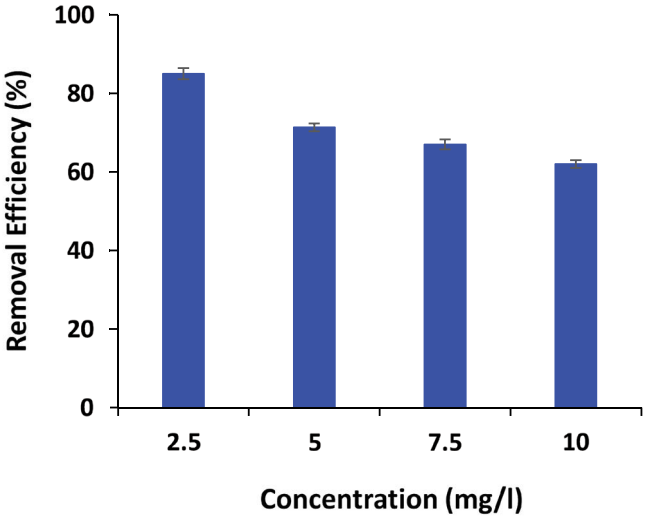

Fig. 10. Effect of initial herbicide concentration on the process performance (Ce.ZnO dose = 0.15 g/L; time = 90 min; sunlight).

Table 1
Comparison of different systems of photocatalytic degradation of 2,4-D

Process	Photocatalyst	Time (min)	pH	Removal (%)	Reference
Visible light photocatalytic decomposition	20% $ZnIn_2S_4$/g-C_3N_4	100	3–4	90	[41]
Visible light–induced photocatalytic degradation	WO_3 (95%)/$NaNbO_3$	90	–	67	[42]
Photocatalytic degradation	TiO_2/BiOBr/Bi_2S_3/AC	90	3	98	[43]
Photocatalytic degradation	Mn-doped ZnO/GO	120	5	65	[27]
Photocatalytic degradation under ultrasonic waves, UV and visible light	Ce.ZnO	90	7	87	This study

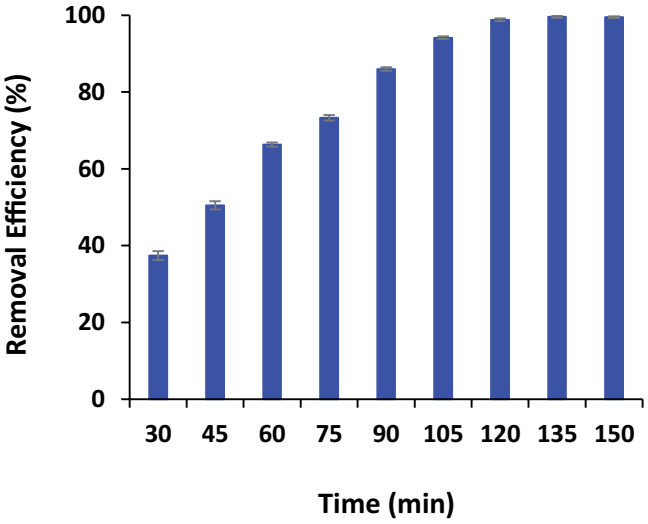

Fig. 11. Effect of contact time on the process performance (initial 2,4-D concentration = 2.5 mg/L; Ce.ZnO dose = 0.15 g/L; sunlight).

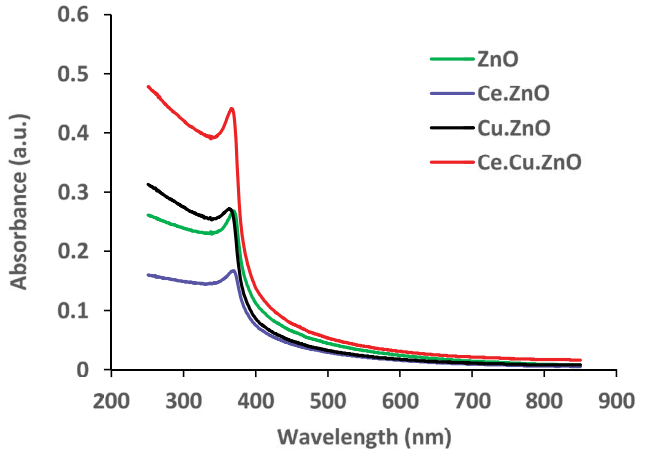

Fig. 12. UV-Vis absorbance spectra of pure ZnO and doped ZnO nanoparticles.

using SEM, XRD, FTIR, AFM, dynamic light scattering (DLS) and zeta potential analyses. According to the results, the Ce.ZnO nanoparticles showed the highest removal efficiency in the presence of visible light for removing herbicides. Therefore, in this study, the Ce.ZnO nanoparticles were used as the most effective nanoparticles in the next experiments. The results indicated that the photocatalytic process showed the highest herbicide removal efficiency at neutral solution pH. Moreover, increasing Ce.ZnO nanoparticle dose increased the photocatalytic removal of 2,4-D herbicide. The results implied that the photocatalytic efficiency increased over contact time. While increasing the initial concentration of 2,4-D herbicide decreased the efficiency of the efficiency. We have found that Ce.ZnO nanoparticles in the presence of visible light yielded a suitable degradation of 2,4-D and therefore, it can be used for the removal of a wide range of herbicides from agricultural wastewater.

Acknowledgments

This research was supported by the Environmental Health Research Center, Kurdistan University of Medical Sciences (No. IR.MUK.REC.1396.192). The authors would like to thank the Kurdistan University of Medical Sciences for its financial support.

References

[1] V.O. Njoku, M. Asif, B.H. Hameed, 2,4-Dichlorophenoxyacetic acid adsorption onto coconut shell-activated carbon: isotherm and kinetic modeling, Desal. Water Treat., 55 (2015) 132–141.
[2] J.M. Salman, K.A. Al-Saad, Adsorption of 2,4-Dichlorophenoxyacetic acid onto date seeds activated carbon: equilibrium, kinetic and thermodynamic studies, Int. J. Chem. Sci., 10 (2012) 677–690.
[3] S. Karami, A. Maleki, E. Karimi, H. Poormazaheri, S. Zandi, B. Davari, Y.Z. Salimi, F. Gharibi, E. Kalantar, Biodegradation of 2,4-Dichlorophenoxyacetic acid by bacteria with highly antibiotic-resistant pattern isolated from wheat field soils in Kurdistan, Iran, Environ. Monit. Assess., 188 (2016) 659–667.
[4] S. Rahimi, A. Poormohammadi, B. Salmani, M. Ahmadian, M. Rezaei, Comparing the photocatalytic process efficiency using batch and tubular reactors in removal of methylene blue dye and COD from simulated textile wastewater, J. Water Reuse Desal., 6 (2016) 574–582.
[5] T.A.S. Hashmi, S.K. Menon, Accumulation and distribution of persistent organochlorine pesticides and their contamination of surface water and sediments of the Sabarmati River, India, J. Adv. Environ. Health. Res., 3 (2015) 15–26.
[6] R. Cattaneo, V.L. Loro, R. Spanevello, F.A. Silveira, L. Luz, D.S. Miron, M.B. Fonseca, B.S. Moraes, B. Clasen, Metabolic and histological parameters of silver catfish (*Rhamdia quelen*) exposed to commercial formulation of 2,4-dichlorophenoxiacetic acid (2,4-D) herbicide, Pestic. Biochem. Physiol., 92 (2008) 133–137.
[7] H.M. Gutiérrez-Zapata, K.L. Rojas, J. Sanabria, J.A. Rengifo-Herrera, 2,4-D abatement from groundwater samples by photo-Fenton processes at circumneutral pH using naturally iron present. Effect of inorganic ions, Environ. Sci. Pollut. Res., 24 (2017) 6213–6221.
[8] E.M. Thurman, M.T. Meyer, Herbicide Metabolites in Surface Water and Groundwater, ACS Symposium Series, American Chemical Society, Washington, DC, 1996.
[9] D.W. Parsons, J.M. Witt, Pesticides *in* Groundwater in the United *States* of America: A *Report of a 1988 Survey of State Lead Agencies*, Oregon *State* University Extension Service *Report EM 8406*, 1989.
[10] M. Kida, S. Ziembowicz, P. Koszelnik, Removal of organochlorine pesticides (OCPs) from aqueous solutions using hydrogen peroxide, ultrasonic waves, and a hybrid process, Sep. Purif. Technol., 192 (2018) 457–464.
[11] P. Bhatt, X.F. Zhou, Y.H. Huang, W.P. Zhang, S.H. Chen, Characterization of the role of esterases in the biodegradation of organophosphate, carbamate, and pyrethroid pesticides, J. Hazard. Mater., 411 (2021) 125026, doi: 10.1016/j.jhazmat.2020.125026.
[12] M.T. Uddin, M.Z.B. Mukhlish, M.R.H. Patwary, A novel magnetically separable $CoFe_2O_4/SnO_2$ composite photocatalyst for the degradation of methylene blue dye from aqueous solution, Desal. Water Treat., 212 (2021) 311–322.
[13] H. Hossaini, G. Moussavi, M. Farrokhi, The investigation of the LED-activated FeFNS-TiO_2 nanocatalyst for photocatalytic degradation and mineralization of organophosphate pesticides in water, Water Res., 59 (2014) 130–144.
[14] R. Shokoohi, A. Dargahi, G. Ahmadidoost, M.J. Moradi, Removal of phenol from aqueous solutions using persulfate-assisted, photocatalytic-activated aluminum oxide nanoparticles, J. Adv. Environ. Health. Res., 7 (2019) 203–212.

[15] C.-H. Liao, S.-F. Kang, Y.-W. Hsu, Zero-valent iron reduction of nitrate in the presence of ultraviolet light, organic matter and hydrogen peroxide, Water Res., 37 (2003) 4109–4118.
[16] B. Shahmoradi, K. Soga, S. Ananda, R. Somashekar, K. Byrappa, Modification of neodymium-doped ZnO hybrid nanoparticles under mild hydrothermal conditions, Nanoscale, 2 (2010) 1160–1164.
[17] X.H. Zhao, M. Li, X.D. Lou, Sol–gel assisted hydrothermal synthesis of ZnO microstructures: morphology control and photocatalytic activity, Adv. Powder Technol., 25 (2014) 372–378.
[18] A.A. Mohammed, S.L. Kareem, Enhancement of ciprofloxacin antibiotic removal from aqueous solution using ZnO nanoparticles coated on pistachio shell, Desal. Water Treat., 213 (2021) 229–239.
[19] F.P. Faria, T.M.O. Ruellas, T.R. Giraldi, C.D. Roveri, S.C. Maestrelli, Zinc oxide porous samples obtained by the sacrifice phase technique as an alternative to water depollution: processing and dye photocatalytic potential, Desal. Water Treat., 212 (2021) 359–367.
[20] J. Müslehiddinoğlu, Y. Uludağ, H.Ö. Özbelge, L. Yilmaz, Effect of operating parameters on selective separation of heavy metals from binary mixtures via polymer enhanced ultrafiltration, J. Membr. Sci., 140 (1998) 251–266.
[21] K.M. Lee, C.W. Lai, K.S. Ngai, J.C. Juan, Recent developments of zinc oxide based photocatalyst in water treatment technology: a review, Water Res., 88 (2016) 428–448.
[22] C.L. Bahena, S.S. Martínez, D.M. Guzmán, M. del R.T. Hernández, Sonophotocatalytic degradation of alazine and gesaprim commercial herbicides in TiO_2 slurry, Chemosphere, 71 (2008) 982–989.
[23] N. Aisah, D. Gustiono, V. Fauzia, I. Sugihartono, R. Nuryadi, Synthesis and enhanced photocatalytic activity of Ce-doped zinc oxide nanorods by hydrothermal method, IOP Conf. Ser.: Mater. Sci. Eng., 172 (2017) 012037.
[24] M. Samadi, M. Zirak, A. Naseri, E. Khorashadizade, A.Z. Moshfegh, Recent progress on doped ZnO nanostructures for visible-light photocatalysis, Thin Solid Films, 605 (2016) 2–19.
[25] H.Y. Xu, H. Wang, Y.C. Zhang, W.L. He, M.K. Zhu, B. Wang, H. Yan, Hydrothermal synthesis of zinc oxide powders with controllable morphology, Ceram. Int., 30 (2004) 93–97.
[26] H. Sowa, H. Ahsbahs, High-pressure X-ray investigation of zincite ZnO single crystals using diamond anvils with an improved shape, J. Appl. Crystallogr., 39 (2006) 169–175.
[27] R. Ebrahimi, M. Mohammadi, A. Maleki, A. Jafari, B. Shahmoradi, R. Rezaee, M. Safari, H. Daraei, O. Giahi, K. Yetilmezsoy, S.H. Puttaiah, Photocatalytic degradation of 2,4-Dichlorophenoxyacetic acid in aqueous solution using Mn-doped ZnO/graphene nanocomposite under LED radiation, J. Inorg. Organomet. Polym. Mater., 30 (2020) 923–934.
[28] B. Subash, B. Krishnakumar, R. Velmurugan, M. Swaminathan, M. Shanthi, Synthesis of Ce co-doped Ag–ZnO photocatalyst with excellent performance for NBB dye degradation under natural sunlight illumination, Catal. Sci. Technol., 2 (2012) 2319–2326.
[29] G.A. Al-Dahash, Q.M. Salman, M.F. Haddawi, Study the effect of copper (Cu) doping on the structure properties of zinc oxide (ZnO) prepared by using pulsed laser deposition (PLD), J. Kerbala Univ., 15 (2017) 87–95.
[30] Ö.A. Yıldırım, H.E. Unalan, C. Durucan, Highly efficient room temperature synthesis of silver-doped zinc oxide (ZnO:Ag) nanoparticles: structural, optical, and photocatalytic properties, J. Am. Ceram. Soc., 96 (2013) 766–773.
[31] G. Asgari, A. Seidmohammadi, M. Bagheri, S. Chavoshi, Evaluating the efficiency of dye removal from textile industry wastewater using the titanium dioxide photocatalytic process under UV-LED light irradiation: a case study, Hamadan Nakh Rang Factory, J. Clin. Med., 24 (2017) 143–151.
[32] M. Ahmadi Moghadam, N. Jaafarzadeh Haghighifard, S. Mirali, S. Jorfi, F. Dinarvand, N. Alavi, Efficiency study on nanophotocatalytic degradation and detoxification of C.I. direct blue 86 from aquatic solution using UVA/TiO_2 and UVA/ZnO, J. Mazandaran Univ. Med. Sci., 26 (2016) 145–159.
[33] G. Riegel, J.R. Bolton, Photocatalytic efficiency variability in TiO_2 particles, J. Phys. Chem., 99 (1995) 4215–4224.
[34] I.K. Konstantinou, T.A. Albanis, TiO_2-assisted photocatalytic degradation of azo dyes in aqueous solution: kinetic and mechanistic investigations: a review, Appl. Catal., B, 49 (2004) 1–14.
[35] M. Behnajady, N. Modirshahla, R. Hamzavi, Kinetic study on photocatalytic degradation of C.I. acid yellow 23 by ZnO photocatalyst, J. Hazard. Mater., 133 (2006) 226–232.
[36] L. Sanchez-Prado, R. Barro, C. Garcia-Jares, M. Llompart, M. Lores, C. Petrakis, N. Kalogerakis, D. Mantzavinos, E. Psillakis, Sonochemical degradation of triclosan in water and wastewater, Ultrason. Sonochem., 15 (2008) 689–694.
[37] E.D. Fard, A.J. Jafari, R.R. Kalantari, M. Gholami, A. Esrafili, Photocatalytic removal of aniline from synthetic wastewater using ZnO nanoparticle under ultraviolet irradiation, Iran. J. Health Environ., 5 (2012) 167–178.
[38] F.D. Mai, C.C. Chen, J.L. Chen, S.C. Liu, Photodegradation of methyl green using visible irradiation in ZnO suspensions: determination of the reaction pathway and identification of intermediates by a high-performance liquid chromatography-photodiode array-electrospray ionization-mass spectrometry method, J. Chromatogr. A, 1189 (2008) 355–365.
[39] M. Qamar, M. Muneer, A comparative photocatalytic activity of titanium dioxide and zinc oxide by investigating the degradation of vanillin, Desalination, 249 (2009) 535–540.
[40] D.F. Ollis, E. Pelizzetti, N. Serpone, Destruction of water contaminants, Environ. Sci. Technol., 25 (1991) 1522–1529.
[41] P.X. Qiu, J.H. Yao, H. Chen, F. Jiang, X.C. Xie, Enhanced visible-light photocatalytic decomposition of 2,4-dichlorophenoxyacetic acid over $ZnIn_2S_4$/g-C_3N_4 photocatalyst, J. Hazard. Mater., 317 (2016) 158–168.
[42] E.J. Hernández-Moreno, A. Martínez de la Cruz, L. Hinojosa-Reyes, J. Guzmán-Mar, M.A. Gracia-Pinilla, A. Hernández-Ramírez, Synthesis, characterization, and visible light–induced photocatalytic evaluation of WO_3/$NaNbO_3$ composites for the degradation of 2,4-D herbicide, Mater. Today Chem., 19 (2021) 100406, doi: 10.1016/j.mtchem.2020.100406.
[43] N. Alikhani, M. Farhadian, A. Goshadrou, S. Tangestaninejad, P. Eskandari, Photocatalytic degradation and adsorption of herbicide 2,4-dichlorophenoxyacetic acid from aqueous solution using TiO_2/BiOBr/Bi_2S_3 nanostructure stabilized on the activated carbon under visible light, Environ. Nanotechnol. Monit. Manage., 15 (2021) 100415, doi: 10.1016/j.enmm.2020.100415.
[44] G.R. Dillip, A.N. Banerjee, V.C. Anitha, B. Deva Prasad Raju, S.W. Joo, B.K. Min, Oxygen vacancy-induced structural, optical, and enhanced supercapacitive performance of zinc oxide anchored graphitic carbon nanofiber hybrid electrodes, ACS Appl. Mater. Interfaces, 8 (2016) 5025–5039.
[45] V. Bharathi, M. Sivakumar, R. Udayabhaskar, H. Takebe, B. Karthikeyan, Optical, structural, enhanced local vibrational and fluorescence properties in K-doped ZnO nanostructures, Appl. Phys. A, 116 (2014) 395–401.
[46] M. Abdennouri, A. Elhalil, M. Farnane, H. Tounsadi, F.Z. Mahjoubi, R. Elmoubarki, M. Sadiq, L. Khamar, A. Galadi, M. Baâlala, M. Bensitel, Y. El Hafiane, A. Smith, N. Barka, Photocatalytic degradation of 2,4-D and 2,4-DP herbicides on Pt/TiO_2 nanoparticles, J. Saudi Chem. Soc., 19 (2015) 485–493.
[47] H. Lee, S.H. Park, Y.-K. Park, S.-J. Kim, S.-G. Seo, S.J. Ki, S.-C. Jung, Photocatalytic reactions of 2,4-dichlorophenoxyacetic acid using a microwave-assisted photocatalysis system, Chem. Eng. J., 278 (2015) 259–264.